Published in final edited form as:
J Immunother. 2011 June ; 34(5): 457–467. doi:10.1097/CJI.0b013e31821dcba5.

Induction of Specific Cellular and Humoral Responses against Renal Cell Carcinoma after Combination Therapy with Cryoablation and Granulocyte-Macrophage Colony Stimulating Factor: A Pilot Study

Archana Thakur[1,*], **Peter Littrup**[2], **Elyse N. Paul**[1], **Barbara Adam**[2], **Lance K. Heilbrun**[1], and **Lawrence G. Lum**[1,3,4]

[1]Department of Oncology, Wayne State University and Karmanos Cancer Institute

[2]Department of Radiology, Wayne State University and Karmanos Cancer Institute

[3]Department of Medicine, Wayne State University and Karmanos Cancer Institute

[4]Department of Immunology and Microbiology, Wayne State University and Karmanos Cancer Institute

Abstract

Cryotherapy offers a minimally invasive treatment option for the management of both irresectable and localized prostate, liver, pulmonary and renal tumors. The anti-neoplastic effects of cryotherapy are mediated by direct tumor lysis and by indirect effects such as intracellular dehydration, pH changes, and microvascular damage resulting in ischemic necrosis. In this study, we investigated whether percutaneous cryoablation of lung metastasis from renal cell carcinoma (RCC) in combination with aerosolized granulocyte-macrophage colony stimulating factor (GM-CSF) can induce systemic cellular and humoral immune responses in 6 RCC patients. Peripheral blood mononuclear cells (PBMC) were sequentially studied up to 63 days post cryoimmunotherapy (CI). PBMC from pre and post CI were phenotyped for lymphocyte subsets and tested for cytotoxicity and IFNγ Elispots directed at RCC cells. Humoral responses were measured by *in vitro* antibody synthesis assay directed at RCC cells. The immune monitoring data showed that CI induced tumor specific CTL, specific *in vitro* anti-tumor antibody responses, and enhanced Th_1 cytokine production in 4 out of 6 patients. More importantly, the magnitude of cellular and humoral anti-tumor response appears to be associated with clinical responses. These pilot data show that CI can induce robust and brisk cellular and humoral immune responses in metastatic RCC patients, but requires further evaluation in optimized protocols.

Keywords

Cryoablation; Cryoimmunotherapy; renal cell carcinoma; lung metastasis; peripheral blood mononuclear cells

[*]**Corresponding Author:** Department of Oncology Barbara Ann Karmanos Cancer Institute, Wayne State University School of Medicine, 731 Hudson Webber Cancer Research Center, 4100 John R., Detroit, MI 48201 thakur@karmanos.org Tel. #:313-576-8321 Fax #: 313-576-8923 .

Financial Disclosure All authors have declared no financial conflicts of interest in regards to this work.

Introduction

Cryotherapy, or cryoablation, has been used for many years to treat cancers in different organ systems using an open surgical approach. The most compelling evidence for using cryotherapy comes from several large studies demonstrating targeted cryoablation of prostate cancer[1-3]. Encouraging clinical outcomes for local disease control in prostate cancer patients[1] led to enthusiastic support for both laparoscopic[4] and percutaneous[5] renal cryotherapy, as well as and pulmonary cryotherapy[6]. Although cryotherapy alone is sufficient to stimulate local and regional immune responses, it is insufficient to induce systemic immune responses. Increased local and regional immune responses such as increased tumor antigen uptake by dentritic cells (DC), upregulation of CD80 expression on DC, increased numbers of tumor antigen positive DCs in the tumor draining lymph nodes (TDLN) and increased tumor specific T-cells responses were evidenced in the murine model of melanoma[7-10] and breast cancer[11, 12]. Si et al. showed that cryoablation of prostate cancer resulted in significantly higher levels of TNF-α, IFN-γ, Th_1/Th_2 ratio and increased tumor specific T-cell response 4 weeks after cryoablation but responses were not sufficiently maintained to prevent cancer relapse[13]. Synergistic and systemic effects were shown when cryoablation was combined with immune modulators. Udagawa, et al[14]. showed that cryoablative pretreatment enhances the efficacy of dendritic cells vaccine stimulated with BCG-CWS *ex vivo*, resulting in the induction of tumor-specific $CD8^+$ T cells responsible for the *in vivo* tumor regression of both treated and remote untreated tumors. Efficacy of cryoablation-induced *in vivo* vaccination was further improved by the addition of unmethylated cytosine-phosphate-guanine (CpG) oligonucleotides (ODNs) or depletion of T-regulatory cells[7, 14]. Cryoablation combined with peritumoral injection of immune adjuvant CpG showed increased tumor specific IFN-γ^+ cells predominantly in the tumor-draining lymph nodes and protected ~90% of all mice after re-challenging with a lethal dose of melanoma tumor cells in tumor-free mice after 40 days[10]. Another study showed presence of OVA-specific $CD8^+$ T-cells in B16OVA tumors indicating that cryoablation plus CpG-ODN results in synergistically improved DC functions and development of OVA-specific T-cells[9]. Increased serum Th1/Th2 ratio was observed in the immune reactive group compared to local effect group in 13 patients with irresectable hepatic tumors treated with percutaneous cryosurgery[15].

Most of the thermal-based methods of tumor destruction including radiofrequency ablation, laser or focused ultrasound exert hyperthermic effects and differ in mode of tumor destruction compared to hypothermic based-cryoablation methods[16-18]. Cryoablation causes most cells to undergo ischemic necrosis whereas cells at the periphery of the ice ball undergo programmed cell death, and majority of the cryo-released antigens are non-denatured intact antigens[19, 20]. Recent animal studies show that cryotherapy is appreciably better than heat-based ablation for immune stimulation[7, 9, 21]. den Brok *et al* compared conventional *ex-vivo* loaded DC vaccine with cryoablated or radiofrequency ablated tumors as a source for *in vivo* DC loading and showed higher numbers of antigen loaded DC in tumor draining lymph nodes after cryoablation when compared to those found after radiofrequency ablation or conventional DC vaccine[7].Tumor antigens in necrotic debris, apoptotic bodies, or lysates derived from tumor cells can be processed and presented to naïve T-cells by DC[22, 23]. Combination of available immune drugs, such as GM-CSF with percutaneous pulmonary cryotherapy may allow monitoring of immune effects and documentation of continued low morbidity when combined.

GM-CSF is the most potent and well-studied adjuvant approved for human use[24] and the only agent that has been delivered as an aerosol. The advantages of aerosol therapy for immunomodulation include low systemic toxicity, high pulmonary drug concentration, increased lymphatic absorption, home administration and highly focused activation of

macrophages and lymphocytes[25]. Multiple cytokines have been utilized in aerosol formulation but GM-CSF has been the prime candidate for induction of an "*in vivo* dendritic cell vaccine"[24, 25]. Combination of immune modulator, such as GM-CSF with percutaneous pulmonary cryotherapy may induce measurable immune responses and allow monitoring of immune effects. In this study, we investigated whether percutaneous cryotherapy in combination with GM-CSF can induce systemic and cellular and humoral immune responses to pulmonary metastases from RCC. GM-CSF was chosen because it is a well-known immune adjuvant[24, 26, 27].

Materials and Methods

Study design and patients

Patients with pulmonary metastases from any primary were eligible. Six of the 8 registered patients had pulmonary metastases from primary RCC, 1 patient from chondrosarcoma, and 1 patient from esophageal carcinoma. In this report, we are presenting data only from the 6 metastatic RCC (mRCC) patients. Patient characteristics are summarized in Table 1. The Institutional Review Board of Wayne State University approved this protocol. All patients underwent the informed consent process and signed consent forms in compliance with HIPAA guidelines.

The schema for the protocol is summarized in Figure 1. Patients were selected for at least one mass deemed to have unobstructed access (e.g., peripheral or no intervening central vasculature) and capable of undergoing 2 sessions of cryotherapy for complete tumor coverage. An 18 gauge histology core biopsy was taken through a 17 gauge Trocar needle immediately prior to the placement of at least two small (≤ 2.4 mm) cryo-probes which bracket the periphery of the mass during the same CT-guided procedure session. Placement in probe density according to tumor size has been previously described, emphasizing rapid freeze and cytotoxic temperatures throughout the tumor[528]. Prior to initiating the freeze, an interstitial injection of GM-CSF (250 μg) was administered near the tumor via the guiding 17 gauge Trocar needle used for biopsy. This limits repeated punctures and potentially locks the GM-CSF in place as the ice forms (GM-CSF is not altered by freezing). On the fourth day of post-cryotherapy rest, one week of twice-daily aerosolized GM-CSF (250 μg/dose) was administered followed by three weeks of rest for a total of four weeks before the second treatment cycle was initiated. This follows the same format as the first cycle with the first treated area already showing some cryotherapy-induced necrotic cavitation.

PBMC and serum collection

Blood and serum were collected at the indicated time points in Figure 1, assuming full patient compliance. Whole blood and serum samples were collected prior to therapy and 4 to 6 samples were collected up to 63 days post cryoablation and stored for immune studies. Peripheral blood mononuclear cells (PBMC) isolated from whole heparinized blood by Ficoll-hypaque density gradient centrifugation were cryopreserved until use.

Cell lines

The human RCC cell lines RC-2 and KCI-18 and NK-cell sensitive cell line K562 were maintained in RPMI-1640 culture medium (Lonza Inc., Allendale, NJ) supplemented with 10% fetal bovine serum (FBS) (Lonza Inc., Allendale, NJ), 2 mM L-glutamine (Invitrogen, Carlsbad, CA), 50 units/ml penicillin, and 50 μg/ml streptomycin (Invitrogen, Carlsbad, CA). These cells served as *in vitro* target cells for cytotoxicity assays, and sources for tumor antigens for interferon-gamma (IFN-γ) EliSpots and *in vitro* antibody synthesis and detection.

Assessment of immune responses

Cytotoxicity assay—Cytotoxic T-lymphocyte (CTL) response to RCC was evaluated in PBMC to assess the specific and non-specific target killing by chromium (^{51}Cr) release assay in 96-well flat-bottomed microtiter plates as previously described [29]. Briefly, patient PBMC were plated in triplicate onto target cells (4×10^4 cells/well by mixing equal numbers of RC-2 and KCI-18 cells) at effector/target (E:T) ratios of 10:1, 5:1, and 2.5:1. ^{51}Cr release was measured after 18 hours and percent cytotoxicity was calculated using the following formula: (experimental cpm -spontaneous cpm) / (maximum cpm - spontaneous cpm) × 100.

EliSpots for IFN-γ-secreting T cells—PBMC were tested for IFNγ secreting T-cells (a surrogate marker for CTL and T helper activity) using EliSpots assay. IFNγ secreting T-cells were assessed after an 18 hour exposure to the specific or non-specific cell lines at E:T of 10:1 in EliSpot plates. Briefly, 96-well plates (BD Biosciences San Jose, CA) were coated with purified anti-human IFNγ antibodies (BD Biosciences San Jose, CA). After washing and blocking with RPMI 10% FBS, appropriate numbers of specific or non-specific cells were added to the plates and incubated overnight at 37°C. Plates were washed with deionized water prior to washing with PBS/0.05% Tween-20 and incubated with IFNγ-specific antibody conjugated to horseradish peroxidase (HRP) (BD Biosciences San Jose, CA). The assay was developed with 3-amino-9-ethylcarbazole (AEC) as a chromogenic substrate (Becton Dickinson), EliSpots were captured and counted on a CTL Immunospot Counter (Cellular Technology Ltd, Shaker Heights, OH) using Immunospot software version 4 (Cellular Technology Ltd, Shaker Heights, OH).

Development of an in vitro model for assessing the humoral immune response—PBMC were washed 5-6 times to remove passive serum antibodies prior to plating in co-cultures for the induction of specific anti-RCC antibody production. One million PBMC were co-cultured with 5 μg/ml CpG-B, or control CpG oligonucleotide (ODNs) (CpG B [2006, TCG TCG TTT CGT CGT TTT GTC GTT] or CpG control DNA [TGC TGC TTT TGT GCT TTT GTG CTT] purchased from Cooley Parmaceutical group (CA). ODNs were used at 5 μg/ml concentration based on pre-titrated optimal antibody responses of PBMC.

Cultures were exposed to RC-2+KCI-18 cells (40,000 cells/well) for 48 h, then non-adherent co-culture suspensions were removed from the plates on day 2 and re-plated on a new plate and incubated for 14 days. Cultures were set up in 250 μl RPMI 1640 medium supplemented with 10% fetal bovine serum, antibiotics, and L-glutamine. Cells were also supplemented with IL-2 every 3rd day (100 IU/10^6 cells). Control cultures were kept in medium without CpG or cancer cells. Supernatants were collected at day 14 and assayed for RC-2+KCI-18 specific antibodies by enzyme linked immunosorbent assay (ELISA).

Antibody detection by ELISA—Tumor-specific antibodies (Ab) were identified by a cell-based ELISA as described previously [30]. RC-2 and KCI-18 were plated in flat-bottomed 96 well plates at a concentration of 50,000 cells/well. Cells were allowed to settle and spread at room temperature for 30 minutes, supernatant were removed, and plates were stored at −20°C. Prior to use, cells were fixed with absolute ethanol at 4°C for 10 minutes followed by blocking with 1% bovine serum albumin (BSA) and 1% normal goat serum (NGS) in PBS with 0.05% Tween 20 (PBST). Serial dilutions of supernatants (sups) for co-cultures for the induction of *in vitro* specific antibody synthesis or serum were placed into the wells to bind to tumor antigens on the fixed tumor cells. After 1 h incubation at 37°C, the plate was washed and HRP conjugated goat anti-human IgG was added and incubated for another 30 minutes at 37°C. Plates were developed by adding 3,3′,5,5′-tetramethylbenzidine (TMB)

substrate (Pierce Bioscience, Rockford, IL) for 10-15 minutes followed by the addition of 2 N H_2SO_4 to stop the reaction. Developed plates were read on a Tecan microplate reader (Tecan, Durham, NC) at a wavelength of 450 nm. The amount of antibody binding to the tumor antigens was calculated from a standard curve generated by known amounts of antibody (anti-human EGFR,) bound to a fixed number of tumor cells. Culture supernatants containing just PBMC consistently produced <15 ng/ml of antibodies.

Flow cytometry—PBMC (1×10^5) were washed 3x with phosphate buffered saline (PBS) + 0.2 % BSA and stained for 30 minutes at 4°C with anti-CD3-FITC/PE/APC, anti-CD4-FITC/PE/APC, anti-CD45RO-APC, anti-CD8-PerCP/APC, anti-CD56-PerCP, anti-CD16-PE, anti-CCR7-PE, anti-CD25-PE antibodies (BD Biosciences, San Jose, CA) at optimal concentrations. Three or Four-color data acquisition was performed with a flow cytometry (BD Biosciences San Jose, CA). Data analysis was performed using FacsDiva forward versus side-scatter gating on viable lymphocytes.

Measurement of cytokine secretion—Serum cytokines were quantitated in patient serum collected at pre- and post-cryoablation immune monitoring time points using 25-plex human cytokine Luminex Array (Invitrogen, Carlsbad, CA) in Bio-Plex system (Bio-Rad Lab., Hercules, CA) according to the manufacturer's instructions. The multiplex panel include interleukin 1β (IL-1β), IL-1 receptor antagonist (Ra), IL-2, IL-2R, IL-4, IL-5, IL-6, IL-7, IL-8, IL-13, IL-17, tumor necrosis factor (TNF-α), interferon-alpha (IFN-α), IFN-γ, GM-CSF, Macrophage inhibitory protein (MIP)-1α, MIP-1β, interferon-inducible protein (IP)-10, MIG, Eotaxin, Regulated on Activation Normal T Cell Expressed and Secreted (RANTES) and Monocyte chemotactic protein (MCP)-1. The limit of detection for these assays is < 10 pg/mL based on detectable signal of > 2 fold above background (Bio-Rad). Cytokine concentration was automatically calculated by the BioPlex Manager Software (Bio-Rad), which uses a standard curve derived from recombinant cytokine standards.

Clinical responses—This study was not designed to assess or correlate outcomes of CI with clinical outcomes of tumor size and/or patient disease burden. As such, standard definitions of complete and partial responses (CR and PR) had to be slightly modified to reflect ablation scar resolution[5, 6] during the time course of 6 and 12 month clinical follow-up. Namely, a CR was defined as involution of the prior tumor and/or ablation site to only a thin, non-enhancing scar within the pulmonary parenchyma on enhanced chest CT. A PR was defined as incomplete resolution of an otherwise thoroughly hypovascular resolving ablation zone which had reached a diameter smaller than the original tumor size. Stable disease (SD) reflects no significant change in size of ablation site and/or overall tumor burden, while the standard definition for progressive disease (PD) remains as evidence of neTw or growing tumors.

Statistical analyses—Since the sample sizes were very small, only descriptive statistical graphics were needed to present the data, including dot plots and line plots. In the dot plots, the median of the distribution was marked with a dash. Analyses were performed using GraphPad Prism version 7.00 for Windows (GraphPad Software, San Diego, CA).

Results

Specific cytotoxic activity observed in patients PBMC after cryo-immunotherapy

In order to determine whether CI induced the development of tumor-specific CTL, PBMC were tested for cytotoxicity against two renal cell carcinoma cell lines RC-2 and KCI-18. Figure 2A (Upper panel) shows an apparent increase in specific cytotoxicity mediated by PBMC directed at RC-2+KCI-18 RCC cells mixed at equal ratio. In 4 of 6 patients peak

cytotoxicity ranged from 7 to 30 % at E:T of 10:1 at day 11 post cryoimmunotherapy (postCI) compared to pre cryoimmunotherapy (preCI) PBMC. Although there were fluctuations between time points, maximum specific cytotoxicity was at day 11 and the cytotoxicity persisted up to 63 days, ranging from 5 to 25% (Figure 2A, Upper panel). NK cell mediated cytotoxicity also increased against NK sensitive-K562 cells in all four patients who also showed increased specific target cell killing in postCI PBMC samples compared to preCI PBMC. Two out of four patients did not show any specific target killing also did not show any NK cell mediated killing (Figure 2A, Lower panel). Patients that showed increased specific and NK cell mediated cytotoxicity were defined as responding patients (n = 4) and patients that did not exhibit any specific or NK cell mediated killing were defined as non-responding patients (n = 2). Both, specific and NK mediated cytotoxicity were apparently higher in responding patients compared to non-responding patients. These data show that the specific cytotoxicity by PBMC persisted up to 2 months postCI in responding patients.

Cryo-immunotherapy induced IFNγ secreting T- cells

The number of IFNγ secreting T-cells was measured by a direct EliSpots at 10:1 E:T ratio in 6 RCC patients to define the kinetics of the CTL responses from preCI to day 63 post CI (Figure 2B). Sufficient cryopreserved PBMC at the serial time points from each patient were thawed and tested for EliSpots. EliSpots ranging from 20–-400 cells/10^6 PBMC preCI increased 2-4 fold to 50–1,600 IFNγ EliSpots/10^6 PBMC between day 11 to day 63 postCI. The median (481) number of IFNγ secreting T cells was higher in responding patients compared to non-responding patients (140) at all time points postCI. Figure 2B shows the tumor-specific (Upper panel), NK cell specific (Middle panel), and unstimulated EliSpot responses (Bottom panel) as a function of days after CI. No responses were observed to a non-small cell lung cancer cell line (irrelevant control, data not shown).

Induction of in vitro specific anti-tumor antibody responses

In order to determine whether PBMC contained memory B cells that had been “immunized” by CI, we tested PBMC in an *in vitro* antibody synthesis assay before and after CI in all six mRCC patients. PBMC were co-cultured with RC-2 + KCI-18 in the presence or absence of CpG ODN for 14 days. All responding patients showed elevated antibody levels on day 32 and 42 post therapy (0-81 ng/ml pre-therapy *vs.* 50-150 ng/ml post-therapy) in the presence of CpG ODNs (Fig. 2C). Supernatants of co-cultures from non-responding patients showed lower levels of *in vitro* antibody synthesis at day 32 or day 42 postCI compared to the responding patients. Specific antibody synthesis by PBMC provides evidence for the development of tumor specific T-helper activity for antibody production. No antibody was detected in the culture supernatants tested against irrelevant control Daudi cell line (data not shown).

Specific antibody response observed in patient serum

To determine whether CI induced *in vivo* humoral immune responses to RCC, serum samples were analysed for antibodies against RCC cells in one responding patient and one non-responding patient. Increased anti-RC-2+KCI-18 serum antibodies were present in both patients postCI (Figure 2D). Both patients showed higher antibody titers to RCC cells postCI compared to preCI serum samples ranging from (1000 ng/ml to 4500 ng/ml).

Cryoimmunotherapy induced effector memory T-cells

To address the T cell responses against mRCC *in vivo*, PBMC from pre and postCI were phenotyped for $CD4^+$, $CD8^+$, $CD4^+/CD25^{+high}$ T cells (T_{regs}), NK cells, and effector memory T cells ($T_{EM,}$ CD8/CD45RO/$CCR7^-$). Phenotypic analysis was done in responding

and non-responding patients at pre and various postCI time points to determine the kinetics of change in T and NK cell population in PBMC. Non-responding patients showed transient decreases in the proportion of all T-cell population ($CD4^+$, $CD8^+$ and, T_{EM}) that recovered by day 11 postCI (Figs. 3A, 3B and 3C). All responding patients showed consistently low numbers of T_{reg} cells compared to non-responding patients (Figure 3D). No difference in the proportions of $CD4^+$, $CD8^+$ and, T_{EM} cells were observed from day 11 to day 63 between responding and non-responding patients. NK cell population increased transiently at day 1 postCI in responding patients compared to PreCI and non-responding patients (Data not shown).

Cryoimmunotherapy induced cytokine response

Next, we examined whether cryoablation would induce endogenous cytokine and chemokine responses that could be detected in the serum. Since serum was only collected from one responding patient and one non-responding patient due to protocol restrictions, cytokine and chemokine profiles were tested in only those two patients (one responder and one non-responder). Proinflammatory cytokines such as IL-1β, TNFα and IFNα showed striking differences between the responder and the non-responder mRCC patients. All three cytokines were higher in the responder mRCC patient (IL-1β, 223-395 pg/ml; TNFα 7-14 pg/ml; IFNα,122-180 pg/ml) compared to the non-responding patient (IL-1β, 0-32 pg/ml; TNFα 2-6 pg/ml; IFNα,16-77 pg/ml). Similarly, Th_1 biased cytokines IFN-γ, IL-12, GM-CSF increased in the responding patient compared to the non-responding patient (Fig 4 A). On the other hand, Th_2 cytokines showed no distinct pattern. Levels of IL-10 were very low in both patients except for one time point at which the IL-10 from the non-responding patient transiently increased more than 50 fold compared to the baseline levels (Fig 4 B). IL-4 and IL-15 levels were significantly higher in the responder compared to the non-responder at all postCI time points. Similar to cytokines, chemokine RANTES was higher in the non-responding patient postCI compared to the responding patient (Fig.4 C).

Clinical responses

Out of 6 patients, the 4 responding patients all had clear cell variety of RCC and showed potent, persistent CTL and antibody responses in immune monitoring studies following CI. One of the 2 non-responders had a sarcomatoid variety of RCC, while the other had clear cell carcinoma. Patients with persistent immune responses also showed better clinical outcomes. The CT scans at 63 days or 2 months post and 6 months post cryoablation showed marked shrinkage of ablated tumor masses in all patients, response for non-ablated tumor masses was observed only in one out of six patients (Table 2b). One patient showed a complete response (CR) and three patients showed either partial responses (PRs) or stable disease (SD) at the 2 and/or 6 month follow-up visits (Table 2a and 2b). Two of the patients in this study were not able to fully tolerate the second regimen of aerosolized GM-CSF. Both patients complained of significant shortness of breath during the first cycle and did not receive the aerosolized portion of the second cycle, yet received their second ablation with the interstitial GM-CSF without difficulty. Of these two patients, who did not complete the second cycle, one was responder and one was non-responder.

Discussion

This is the first study to report the induction of cellular and humoral anti-tumor immune responses in patients after combination immunotherapy using cryoablation with GM-CSF to treat pulmonary metastasis of mRCC. Patients received two cycles of CT-guided cryoablation + 250 μg of peri-tumoral GM-CSF followed by twice daily dose of 250 μg of aerosolized GM-CSF as an immune adjuvant. GMCSF is likely to augment DC functions by enhancing uptake, processing, and presentation of tumor antigens released by cryoablation

to naive T-cells leading to the development of a robust systemic immune response against tumor. The advantages of aerosol therapy for immune-modulation, particularly for pulmonary metastasis, include low systemic toxicity, high pulmonary drug concentration, increased lymphatic absorption, home administration, and highly focused delivery/activation of immune cells[25].

Higher specific cytotoxicity in 4 out of 6 patients paralleled high numbers of IFN-γ producing cells, increased Th_1/Th_2 ratio, specific RCC antibody responses, and high NK mediated cytotoxicity suggest an activation of T-, B- and NK cells postCI. These data suggest the effectiveness of CI to induce both cellular and humoral anti-tumor activity in mRCC patients. Out of six patients, two (defined as nonresponders) neither exhibited cytotoxicity against specific targets nor showed induction of RCC specific antibody at any time point postCI. It is noteworthy that the two non-responding patients showed increased proportion of T_{reg} cells early after postCI and a decreased Th_1/Th_2 ratio; these conditions may have been responsible for their non-responsiveness.

Since cytokines and chemokines play critical roles in migration, proliferation, maturation, and activation of immune cells, cytokine and chemokine milieu at the tumor site will shape immune responses. We, therefore, assessed the effect of CI on the cytokine pattern in responding and non-responding patients by multiplex cytokine array. The cytokine/chemokine profiling showed distinct patterns for responders versus non-responders. Predominant cytokines and chemokines were those associated with the inflammation, recruitment, differentiation, and activation of immune cells. The combination cryoablation + GM-CSF therapy led to a significant increase in serum IL-12, IFN-γ, GM-CSF, and IL-4 levels peaking first between days 1 and 11 followed by a second peak at day 32 postCI in responding patient (Figure 4A). Intriguingly, T-cell proliferation related cytokines such as IL-2 and IL-15 also increased 24 h postCI in the responding patient with no detectable levels in the non-responding patient. IL-15 promotes differentiation of $CD8^+$ T-cells into T_{EM} whereas IL-2 directs $CD8^+$ T cells to preferentially differentiate into T_{CM}[31, 32]. We observed a patient with progressive disease who tended toward Th_2-type responses, and a patient with PR who showed a Th_1-polarizing responses postCI, underscoring the importance of Th_1 responses in anti-tumor activity. Our findings are consistent with previous studies showing that high serum cytokine Th_1/Th_2 ratios in responding patients not only had local immune effects but their distal metastatic lesions also became necrotic while non-immune responding patients had high levels of IL-10 before and after CI[33]. However, in our study it is difficult to interpret whether these enhanced immune responses are exclusively due to the combination of CI with GM-CSF since we did not evaluate GM-CSF alone, or cryotherapy alone as controls.

A number of studies have shown potential clinical benefits of image-guided percutaneous cryotherapy over a surgical procedure as a primary intervention for localized disease, irresectable metastases, or as salvage therapy[34-37]. However, there have been no systematic studies to evaluate CI-induced immune responses and their association with clinical responses. Development of immune responses following CI is not only affected by combination of immune adjuvants/vaccines but also by the freeze rate, the total freezing time, the number of freeze-thaw cycles, and the mode of administration of the immune adjuvant. Pulmonary metastases in our study received high cytotoxic freeze rates, which may be important since Sabel *et al.*[11] recently reported that freeze rates can alter immune responses from stimulatory to suppressive in nature. Cryoablation using a high freeze rate resulted in a significant increase in tumor-specific T cells in the tumor draining lymph nodes (TDLN), a reduction in pulmonary metastases, and improved survival. In contrast, cryoablation using a low freeze rate resulted in an increase in regulatory T cells, a significant increase in pulmonary metastases, and decreased survival [11]. Similarly, Nierkens

et al. showed that the route of CpG administration can enhance the *in situ* activation of DC and anti-tumor immunity[10]. Since development of immune response depends upon multiple factors, variability in any of the parameters may change the nature of immune response following cryoablation as seen in previous studies displaying the range of immunological responses[7, 10-12, 38]. Based on our data we propose that "cryoshock" along with the immune-adjuvant properties of GM-CSF not only releases tumor antigens by cryolysing of tumor cells but also induces release of multiple cytokines and chemokines (Fig. 5). CI induced immune milieu leads to the recruitment, differentiation, and activation of immune cells including T-, B-, APCs, and NK cells. Recruited APCs may uptake the tumor antigens and migrate to the regional lymph nodes and present tumor antigens to naïve T-cells resulting in the clonal expansion of tumor specific T- and B-cells. Tumor antigen specific T-cells and B-cells along with the activation of innate immune cells may help eliminate the residual tumor cells at the ablated site as well as at distal sites. Modulating the immunologic milieu prior to cryoablation is also being investigated, particularly in relation to T_{reg} cells in their production of tumor tolerance or blocking anti-tumor functions. Cyclophosphamide has been shown to reduce T_{reg} cells and is being explored in conjunction with cryoablation for patients with metastatic prostate and RCC[39]. Such modulation and improvement of CI protocols will be crucial to effect sustained immune vigilance against tumor recurrence in the future. In spite of encouraging data, this study has two major limitations: 1) the sample size is very small; and 2) the absence of control arm of GM-CSF alone precludes an assessment of the GM-CSF effect independent of cryotherapy.

In summary, our data suggest that CI not only has a direct local anti-tumor effect but also results in the development of systemic immune response. These results suggest that the combination strategy of CI with the immune adjuvant GM-CSF may provide a method for *in situ* immunization in patients against their own tumors and these vaccine responses may lead to persistent clinical responses with optimized CI protocols.

Acknowledgments

This study was partially supported by NIH Cancer Center Support Grant Supplement CA-22453-S1, by NIH Cancer Center Support Grant CA-22453, and R01 092344.

References

1. Bahn DK, Lee F, Badalament R, Kumar A, Greski J, Chernick M. Targeted cryoablation of the prostate: 7-year outcomes in the primary treatment of prostate cancer. Urology. 2002; 60:3–11. [PubMed: 12206842]
2. Lee F, Bahn DK, McHugh TA, Onik GM, Lee FT Jr. US-guided percutaneous cryoablation of prostate cancer. Radiology. 1994; 192:769–76. [PubMed: 8058945]
3. Onik GM, Cohen JK, Reyes GD, Rubinsky B, Chang Z, Baust J. Transrectal ultrasound-guided percutaneous radical cryosurgical ablation of the prostate. Cancer. 1993; 72:1291–9. [PubMed: 7687922]
4. Gill IS, Remer EM, Hasan WA, et al. Renal cryoablation: outcome at 3 years. J Urol. 2005; 173:1903–7. [PubMed: 15879772]
5. Littrup PJ, Ahmed A, Aoun HD, et al. CT-guided percutaneous cryotherapy of renal masses. J Vasc Interv Radiol. 2007; 18:383–92. [PubMed: 17377184]
6. Wang H, Littrup PJ, Duan Y, Zhang Y, Feng H, Nie Z. Thoracic masses treated with percutaneous cryotherapy: initial experience with more than 200 procedures. Radiology. 2005; 235:289–98. [PubMed: 15798173]
7. den Brok MH, Sutmuller RP, Nierkens S, et al. Efficient loading of dendritic cells following cryo and radiofrequency ablation in combination with immune modulation induces anti-tumour immunity. Br J Cancer. 2006; 95:896–905. [PubMed: 16953240]

8. den Brok MH, Sutmuller RP, Nierkens S, et al. Synergy between in situ cryoablation and TLR9 stimulation results in a highly effective in vivo dendritic cell vaccine. Cancer Res. 2006; 66:7285–92. [PubMed: 16849578]
9. den Brok MH, Sutmuller RP, van der Voort R, et al. In situ tumor ablation creates an antigen source for the generation of antitumor immunity. Cancer Res. 2004; 64:4024–9. [PubMed: 15173017]
10. Nierkens S, den Brok MH, Roelofsen T, et al. Route of administration of the TLR9 agonist CpG critically determines the efficacy of cancer immunotherapy in mice. PLoS One. 2009; 4:e8368. [PubMed: 20020049]
11. Sabel MS, Arora A, Su G, Chang AE. Adoptive immunotherapy of breast cancer with lymph node cells primed by cryoablation of the primary tumor. Cryobiology. 2006; 53:360–6. [PubMed: 16973145]
12. Sabel MS, Nehs MA, Su G, Lowler KP, Ferrara JL, Chang AE. Immunologic response to cryoablation of breast cancer. Breast Cancer Res Treat. 2005; 90:97–104. [PubMed: 15770533]
13. Si T, Guo Z, Hao X. Immunologic response to primary cryoablation of high-risk prostate cancer. Cryobiology. 2008; 57:66–71. [PubMed: 18593573]
14. Udagawa M, Kudo-Saito C, Hasegawa G, et al. Enhancement of immunologic tumor regression by intratumoral administration of dendritic cells in combination with cryoablative tumor pretreatment and Bacillus Calmette-Guerin cell wall skeleton stimulation. Clin Cancer Res. 2006; 12:7465–75. [PubMed: 17189420]
15. Osada S, Imai H, Tomita H, et al. Serum cytokine levels in response to hepatic cryoablation. J Surg Oncol. 2007; 95:491–8. [PubMed: 17219394]
16. McGahan JP, Brock JM, Tesluk H, Gu WZ, Schneider P, Browning PD. Hepatic ablation with use of radio-frequency electrocautery in the animal model. J Vasc Interv Radiol. 1992; 3:291–7. [PubMed: 1627876]
17. Singletary SE, Fornage BD, Sneige N, et al. Radiofrequency ablation of early-stage invasive breast tumors: an overview. Cancer J. 2002; 8:177–80. [PubMed: 11999950]
18. Sherar MD, Trachtenberg J, Davidson SR, et al. Interstitial microwave thermal therapy for prostate cancer. J Endourol. 2003; 17:617–25. [PubMed: 14622481]
19. Bischof JC, Coad JE, Hoffmann NE, Roberts KR. Is apoptosis an important mechanism of cryoinjury in vivo? Cryo Letters. 2002; 23:277–8. author reply 9-80. [PubMed: 12391490]
20. Rupp CC, Hoffmann NE, Schmidlin FR, Swanlund DJ, Bischof JC, Coad JE. Cryosurgical changes in the porcine kidney: histologic analysis with thermal history correlation. Cryobiology. 2002; 45:167–82. [PubMed: 12482382]
21. Ravindranath MH, Wood TF, Soh D, et al. Cryosurgical ablation of liver tumors in colon cancer patients increases the serum total ganglioside level and then selectively augments antiganglioside IgM. Cryobiology. 2002; 45:10–21. [PubMed: 12445546]
22. Littrup PJ, Mody A, Sparschu R, et al. Prostatic cryotherapy: ultrasonographic and pathologic correlation in the canine model. Urology. 1994; 44:175–83. discussion 83-4. [PubMed: 8048191]
23. Vaishampayan U, Abrams J, Darrah D, Jones V, Mitchell MS. Active immunotherapy of metastatic melanoma with allogeneic melanoma lysates and interferon alpha. Clin Cancer Res. 2002; 8:3696–701. [PubMed: 12473578]
24. Borrello I, Pardoll D. GM-CSF-based cellular vaccines: a review of the clinical experience. Cytokine Growth Factor Rev. 2002; 13:185–93. [PubMed: 11900993]
25. Anderson PM, Markovic SN, Sloan JA, et al. Aerosol granulocyte macrophage-colony stimulating factor: a low toxicity, lung-specific biological therapy in patients with lung metastases. Clin Cancer Res. 1999; 5:2316–23. [PubMed: 10499599]
26. Pan PY, Li Y, Li Q, et al. In situ recruitment of antigen-presenting cells by intratumoral GM-CSF gene delivery. Cancer Immunol Immunother. 2004; 53:17–25. [PubMed: 12955480]
27. Rao RD, Anderson PM, Arndt CA, Wettstein PJ, Markovic SN. Aerosolized granulocyte macrophage colony-stimulating factor (GM-CSF) therapy in metastatic cancer. Am J Clin Oncol. 2003; 26:493–8. [PubMed: 14528078]
28. Littrup PJ, Jallad B, Chandiwala-Mody P, D'Agostini M, Adam BA, Bouwman D. Cryotherapy for breast cancer: a feasibility study without excision. J Vasc Interv Radiol. 2009; 20:1329–41. [PubMed: 19800542]

29. Grabert RC, Cousens LP, Smith JA, et al. Human T cells armed with Her2/neu bispecific antibodies divide, are cytotoxic, and secrete cytokines with repeated stimulation. Clin Cancer Res. 2006; 12:569–76. [PubMed: 16428502]

30. Lee JC, Cevallos AM, Naeem A, Lennard-Jones JE, Farthing MJ. Detection of anti-colon antibodies in inflammatory bowel disease using human cultured colonic cells. Gut. 1999; 44:196–202. [PubMed: 9895378]

31. Geginat J, Sallusto F, Lanzavecchia A. Cytokine-driven proliferation and differentiation of human naive, central memory, and effector memory CD4(+) T cells. J Exp Med. 2001; 194:1711–9. [PubMed: 11748273]

32. Picker LJ, Reed-Inderbitzin EF, Hagen SI, et al. IL-15 induces CD4 effector memory T cell production and tissue emigration in nonhuman primates. J Clin Invest. 2006; 116:1514–24. [PubMed: 16691294]

33. Amaoka N, Osada S, Kanematsu M, et al. Clinicopathological features of hepatocellular carcinoma evaluated by vascular endothelial growth factor expression. J Gastroenterol Hepatol. 2007; 22:2202–7. [PubMed: 18031381]

34. Silverman SG, Tuncali K, vanSonnenberg E, et al. Renal tumors: MR imaging-guided percutaneous cryotherapy--initial experience in 23 patients. Radiology. 2005; 236:716–24. [PubMed: 16040927]

35. Gupta A, Allaf ME, Kavoussi LR, et al. Computerized tomography guided percutaneous renal cryoablation with the patient under conscious sedation: initial clinical experience. J Urol. 2006; 175:447–52. discussion 52-3. [PubMed: 16406968]

36. Shingleton WB, Sewell PE Jr. Cryoablation of renal tumours in patients with solitary kidneys. BJU Int. 2003; 92:237–9. [PubMed: 12887474]

37. Davol PE, Fulmer BR, Rukstalis DB. Long-term results of cryoablation for renal cancer and complex renal masses. Urology. 2006; 68:2–6. [PubMed: 16857453]

38. Machlenkin A, Goldberger O, Tirosh B, et al. Combined dendritic cell cryotherapy of tumor induces systemic antimetastatic immunity. Clin Cancer Res. 2005; 11:4955–61. [PubMed: 16000595]

39. Sidana A, Chowdhury WH, Fuchs EJ, Rodriguez R. Cryoimmunotherapy in urologic oncology. Urology. 75:1009–14. [PubMed: 19758686]

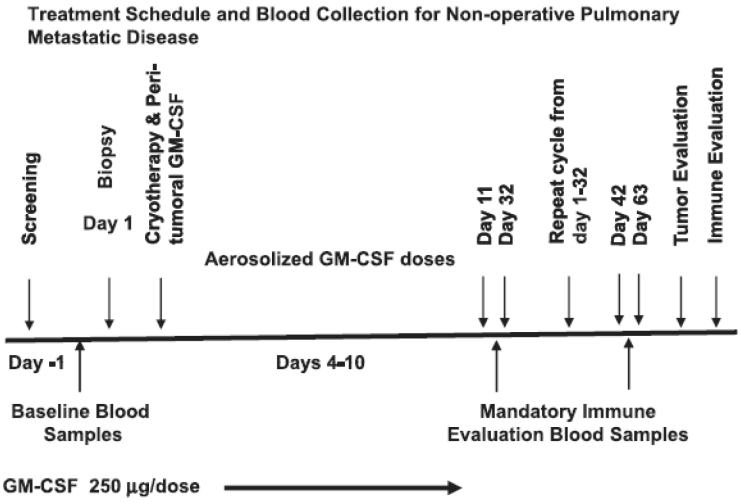

Figure 1.
Treatment schema and blood collection for patients with pulmonary mRCC.

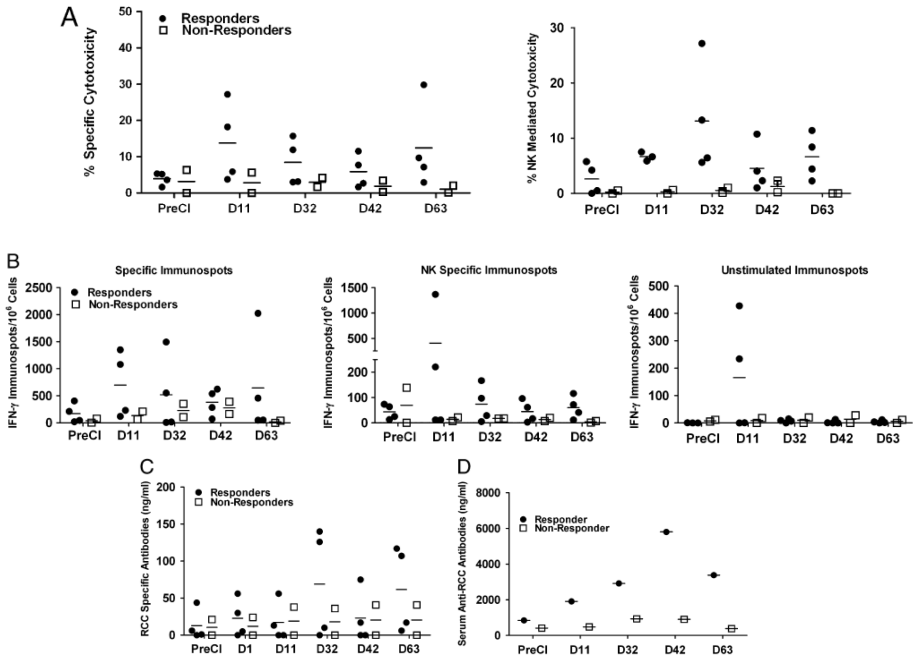

Figure 2. Evidence of tumor specific cytotoxicity, IFN-γ EliSpots and *in vitro* antibody synthesis

A) Upper graph shows specific cytotoxicity (median [marked by a dash] and range) mediated by PBMC from 6 patients at the indicated time points directed at RCC-2+KCI-18. Cytotoxicity was performed at an E:T ratio 10:1 in 4 responding and 2 non-responding mRCC patients. Lower graph shows NK-mediated killing directed at K562 in 4 responding and 2 non-responding mRCC patients. **B)** Shows the IFN-γ Elispots (median and range) produced by PBMC at preCI, days 11, 32, 42, and 63 after CI from 4 responding and 2 non-responding mRCC patients upon 18 h stimulation either with RC-2+KCI-18 (Upper) or K562 (Middle) or left unstimulated (Bottom). **C)** Shows *in vitro* RCC specific antibody synthesis (median and range) by PBMC exposed to RC-2+KCI-18 cells in the presence of CpG. **D)** shows the serum antibody titers against RC-2+KCI-18 in one responding patient and one non-responding patient.

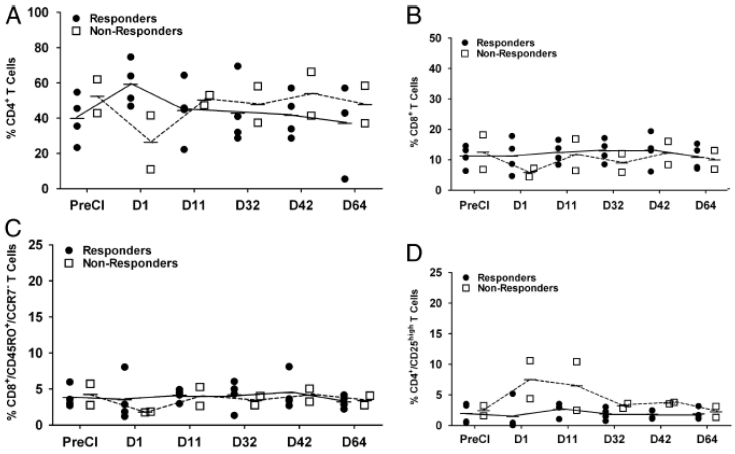

Figure 3. Effect of cryoimmunotherapy on the lymphocyte population

A) Show the percentage of positively immunostained cells for $CD4^+$, **B)** Show the percentage of $CD8^+$, **C)** Show the percentage of $CD8^+T_{EM}$ ($CD45RO^+/CCR7^-$) and **B)** Show the percentage of T_{reg} ($CD4^+/CD25^{+high}$) lymphocyte population in PBMC from 4 responding and 2 non-responding mRCC patients phenotyped by flow cytometry.

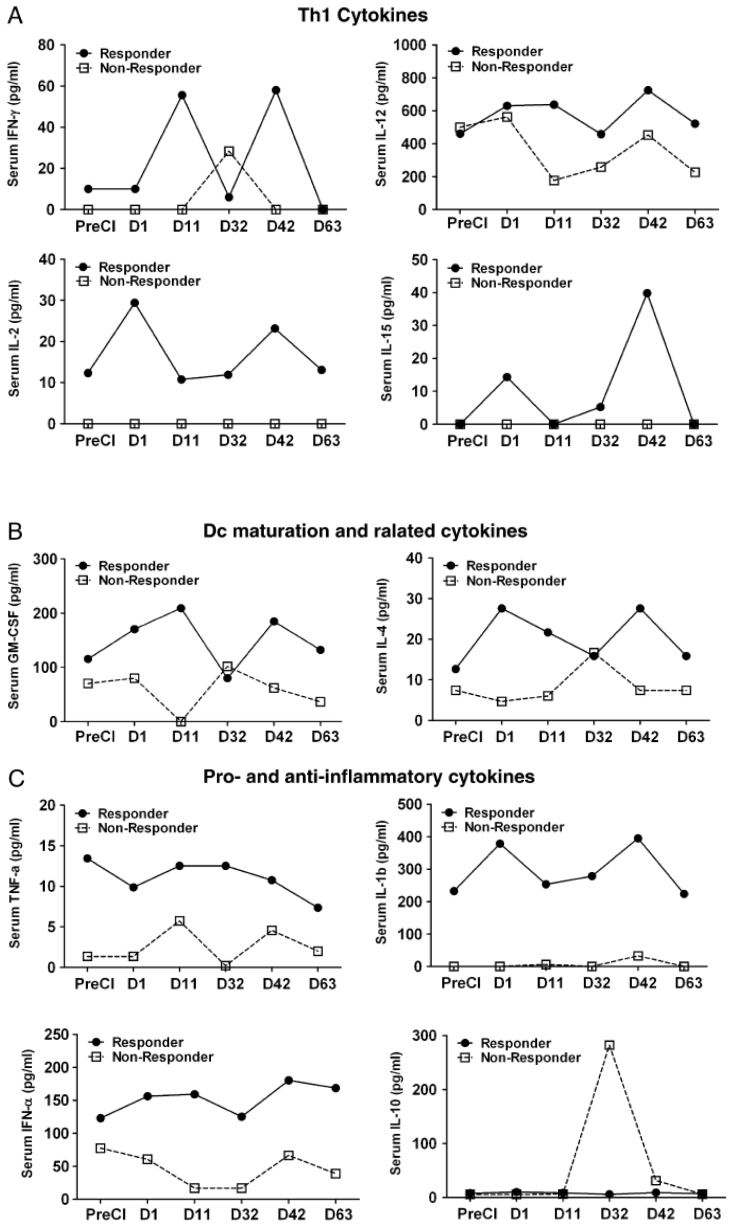

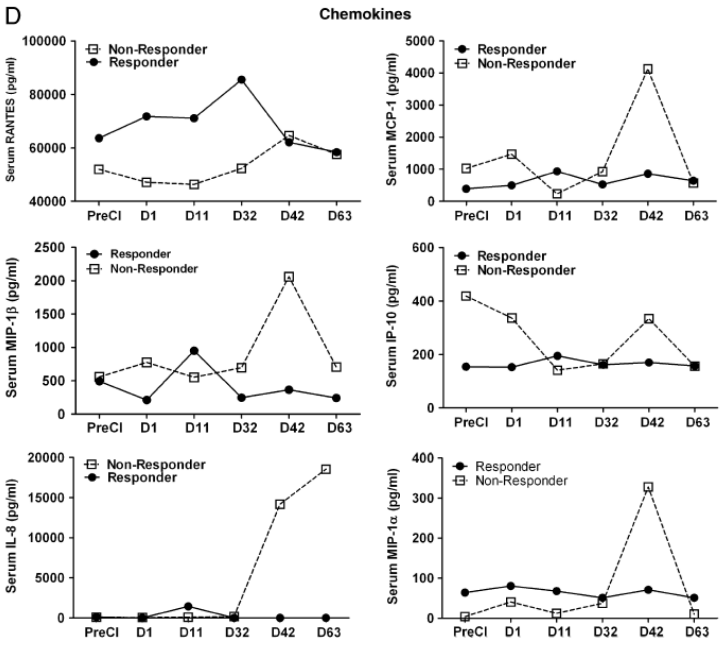

Figure 4. Cytokine/chemokine profile of patient serum

A) Shows serum levels of cytokines, IFN-γ, IL-12, IL-2, IL-15, GM-CSF, and IL-4 at indicated time points postCI. For better visualization of the data, a different scale on the Y-axis was used for each cytokine in one responding patient and one non-responding patient. **B)** Shows serum levels of inflammatory cytokine TNF-α, IL-1β, IFN-α and immune suppressive cytokine IL-10. **C)** Shows the serum levels of chemokines RANTES, MIP-1a, MIP-1b, MCP-1, IP-10 and IL-8 in one responding patient and one non-responding patient.

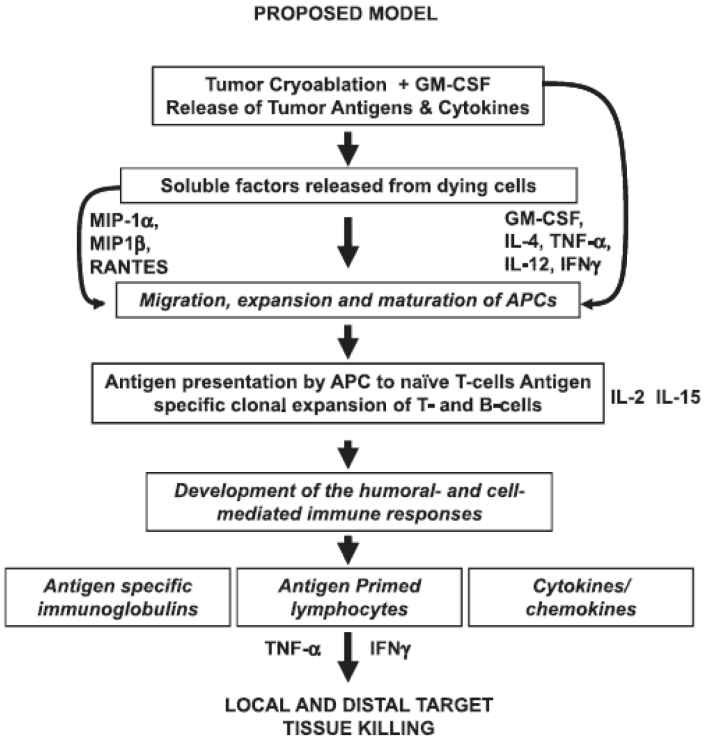

Figure 5. A proposed model of cryoimmunotherapy induced *in vivo* immunization of patients' endogenous immune cells

Tumor antigens and soluble factors released from dying and apoptotic tumor cells induce release of cytokines as a function of cryoimmunotherapy. Cytokines (IL-4 and GM-CSF) can induce maturation and activation of monocytes to DC. Maturation and activated antigen primed DC can process and present antigen to naïve T-cells leading to T- and B-cell interactions (IL-12 and IFN-γ), cell proliferation, and differentiation of T cells supported by IL-2 and IL-15 into tumor specific CTL and T helper cells for specific antibody producing cells.

Table 1

Patient Characteristics

Patients	Primary Tumor Type	Number of Mets	Number of Mets Ablated and Ablation Dates	Nephrectomy/ Cytoreductive Nephrectomy Status	Karnofsky Performance Status	Prior Immuno- or Targeted Therapy
mRCC-1	RCC-clear cell w/sarcomatoid features	4	2 Mets 9/11/2006 and 11/16/2006	Right nephrectomy 3/2006	100	None
mRCC-2	RCC-moderately differentiated	5	2 Mets 1/8/2007 and 3/13/2007	Left nephrectomy 3/2004	100	IL-2
mRCC-3	RCC-clear cell type	4	2 Mets 4/30/2007 and 6/29/2007	Left nephrectomy 3/2005	90	None
mRCC-5	RCC-clear cell type	3	2 Mets 7/9/2007 and 9/10/2007	Left cytoreductive nephrectomy 9/2004	100	Nexavar
mRCC-7	RCC-clear cell type	2	2 Mets 12/15/2008 and 2/27/2009	Right nephrectomy 11/2007	100	Sutent
mRCC-8	RCC-clear cell type	7	2 Mets 3/2/2009 and 5/4/2009	Left cytoreductive nephrectomy	90	None

Table 2a

Clinical responses and immune correlates of 6 mRCC patients following cryoimmunotherapy.

Patients	Clinical Response 6M-post CI	Clinical Response 12M-post CI	Specific % Cytotoxicity*	Specific IgG Response (ng/ml)**	Specific IFN-γ EliSpots/10^6 Cells$	% T_{reg} Population#	Adverse Events
mRCC-1	PD	PD	0	0	63	10.6	Pneumothorax after cryo #1 grade 2 (moderate)
mRCC-2	PR	PR	3.7	5	120	0.11	Pneumothorax after cryo #1 grade 2 (moderate)
mRCC-3	PR	PR	5.8	10	213	5.2	Mild hemoptysis-self limited grade 1 (minor)
mRCC-5	CR	CR	27	126	1080	0.7	No complications
mRCC-7	PD	PD	28	38	209	4.4	Pneumothorax after cryo #1 self limited-no intervention grade 1/ Shortness of Breath
mRCC-8	PR	PR	6	140	1350	0.46	Shortness of Breath

*Day 11;

**Day 32;

$Day 11;

#Day 11;

PR = partial response; CR = complete response; PD=progressive disease.

Table 2b

Tumor regression at day 63 and 6 months post cryoablation.

Patients	Location of two Mets ablated	Ablation zone (Volume in cm^3)	Day 63 (Volume in cm^3)	6M (Volume in cm^3)	Description
mRCC1	RUL	4.5×2.6×3.0cm (35.1)	1.4×1.4×2.1cm (4.1)	1.0×0.3×0.4 cm (0.12)	New and increased pulmonary mets and new perihepatic, right nephrectomy site and right parapsoas
	Left costophrenic angle	4.5×3.0×3.0cm (36)	3.1×1.1×1.3cm (4.43)	2.8×0.7×0.7cm (1.37)	
mRCC2	RUL	4.0×3.7×3.5cm (51.8)	2.5×1.6×1.4cm (5.6)	2×0.8×1.5cm (2.4)	stable right paratracheal and Hilar adenopathy
	paratracheal mass	2.4×2.3×2.0cm (11)	5.5×4.5×5.5cm (136)	5.5×4.6×5.5cm (139)	
mRCC3	LLL	4.8×3.4×4.0cm (65.3)	4.4×2.6×3.0cm (34.3)	2.3×2.5×1.8 cm (10.3)	Increase in left lower nodule, left hilar and subcarinal nodes
	LLL	4.2×3.1×3.1cm (40.3)	3.7×2.2×2.5cm (20.3)	1.5×0.8×1.0 cm (1.2)	
mRCC5	LLL	4.0×3.0×3.5cm (42)	1.7×1.4×1.0 cm (2.4)	resorbed	Slow progression of lung mets, increased right renal mass
	RLL	3.0×4.5×3.0cm (40.5)	2.1×3.0×2.9 cm (18.3)	resorbed	
mRCC7	RLL	4.6×3.0×4.0cm (55.2)	2.6×1.1×2.4 cm (6.8)	resorbed	Increase in hilar node, right lung base increased
	Left costophrenic angle	4.0×3.0×3.0cm (36)	2.6×2.6×2.6 cm (17.6)	1.4×1.1×1.0cm (1.54)	
mRCC8	RLL	4.8×4.2×4.0cm (80.6)	2.6×2.1×2.1cm (11.5)	1.1×1.6×1.2cm (2.1)	Stable (non-ablated) nodules in RML and RUL lung
	RLL	2.6×3.7×3.0cm (28.8)	2.7×4.3×2.1cm (24.4)	2.6×1.7×2.1cm (9.2)	

Mets: Metastases; RUL: Right Upper Lobe; LLL: Left Lower Lobe; RLL: Right Lower Lobe; b/l: bilateral; Parenthesis show the tumor volume in cm^3